Journal of Electronics and Informatics (ISSN: 2582-3825)
www.irojournals.com/iroei/

A Review on Meshing Techniques in Biomedicine

T. V. Smitha[1], Madhura. S[2], K. V. Bhargava Ram[3], Mahalakshmi. M[3]

[1]Department of Mathematics, RV Institute of Technology and Management, Bangalore
[2]Department of Electronics and Communication Engineering, RV Institute of Technology and Management, Bangalore
[3]Department of ISE, RV Institute of Technology and Management, Bangalore

E-mail: [1]smithatv.rvitm@rvei.edu.in, [2]madhu4tulip@gmail.com , [3] kattavenkatab_is19.rvitm@rvei.edu.in, [4]mahalakshmim_is19.rvitm@rvei.edu.in

Abstract

Engineering has a wide range of applications where more detailed and reliable data are needed, one of which is biomedicine. One of the aims of meshing is to use the Finite Element Approach to solve the problem. By analysing and segmenting raw medical imaging data, meshing aids in a better and more precise understanding of the organs and structures of human body. The main goal of this paper is to collect and review the various available methods in meshing. Also, a comparison study of different meshing techniques that are available in biomedicine is performed.

Keywords: Meshing, biomedicine, medical imaging, Finite element method

1. Introduction

Meshing is indeed an important aspect of an engineering simulation process in which complex geometries are broken into simple elements to be applied to the broader field as discrete local approaches. The mesh influences simulation precision, convergence and pace [1]. Finite Element approach reduces degrees of freedom by means of discretization or meshing from infinite to finite nodes and elements. One of the goals of meshing is to solve the problem with Finite Element method (FEM). The domain can be divided into pieces by meshing, each piece of which represents an element [2].

It is a very powerful analysis tool, but its advantage is hampered by the need to generate a mesh, but if it is done manually, it could be prolonged and error prone. For the Finite Element analysis, Delaunay triangulation is often considered [1, 3]. Triangular shape in two dimensional

DOI: https://doi.org/10.36548/jei.2021.4.001
Received: 20.10.2021, received in revised form: 05.11.2021, accepted: 26.11.2021, published: 06.12.2021

and tetrahedral shape in three dimensional are the regular shapes for mesh generation. First step in creating a 3D mesh is Surface (2D) mesh.

The Finite Element Method is also used to solve problems in biomedical and other engineering applications with the aid of mesh generation. The FEM has become an important tool in medical imaging as well. For instance, Computerized Tomography (CT) scans of legs could be meshed in such a way that the orthopaedic modelling could accurately simulate gait, Magnetic Resonance Imaging (MRI) scans of the torso are frequently used in cardiac electro physical modelling, and images of the skull can identify structures of the brain [2, 4].

For simulation purposes, various types of numerical techniques are used in the biomedical field. For example, stress analysis of human skull during head impact or understanding stress distribution in hip implants, etc. Techniques like Computational Fluid Dynamics (CFD) help to gain insight into fluid motion in and around the body. Analysis of blood flow in arteries, simulation of air-flow in the respiratory passages, etc., are some examples of CFD usage in bio-medical field. Thermal analysis is another interesting technique which helps in understanding the heat transfer mechanism between various parts of the body and the external environment. Thermal analysis of cooling of a human heart during cardiac surgery is one such application [2, 5].

1.1 The need for meshes

In most medical applications, the model structure is not simulated using a CAD 3D Software package but ideally generated using patient data-base image analysis. As the consequence, the initiating point of this structure is one or more of MRI or CT volumes. This multiple modal samples could be enrolled and retested, leading to a volumetric scalar or vector image, usually of some hundreds of voxels across each axis [6]. Consider an example that the 1mm isotropic Magnetic Resonance image of the head is roughly 256 x 256 x 256. This is equal to more than 1.6 crores voxels, which in turn prohibits effective computing directly dependent on the segmented or raw image data. Along with this, numerous biomechanical engines need the fragmentation of the mathematically complex body into uncomplicated shaped elements, since the computation is a matrix equation usually based on basic elementary expressions that are well understood [7, 8]. These demands, computational efficiency and geometric decomposition, that encourage to provide basic forms of the anatomy, such as triangles and tetrahedra, a process that is idealized in 2D (shown in Figure-1) and a mesh generation description. The tetrahedral generation refers to unstructured mesh generation in the

communities of mesh generation in comparison to organized mesh that is usually comprised of hexahedron. In medical simulation, the above are typically not used because this form of meshing requires a large amount of manual intervention (unlike tetrahedral meshing, which could be automated). In addition, the partition of a hexahedron will not limit its potential application to more hexahedrons for interactive simulation, although the tetrahedron gradually becomes more tetrahedra. However, hexahedra have been applied for statistical modelling and appears to yield robust numerical effects [9]. For patient-specific emulation, one way to use Hexahedra involves the distribution of specific anatomy to the patient's anatomy that is feasible if the tissue structure is well defined between humans and the non-rigid transformation [16].

Figure 1. Basic processing idealised in 2D of MRI/CT scan image [16].

2. Literature Review

Mesh generator usually generates only single type of element, but the elements can be converted into desired ones. Brick and quadrilateral can be simply converted into voluptuous tetrahedral and triangles respectively (shown in Figure-2). Tetrahedron and triangle might be divided into bricks and quadrilaterals respectively (shown in Figure-3), but they are not shaped well since the angles around the introduced nodes are relatively large. Heighway provides a way to convert the mesh of triangles into mesh of quadrilaterals by merging every two adjacent triangles to a quadrilateral [1, 10].

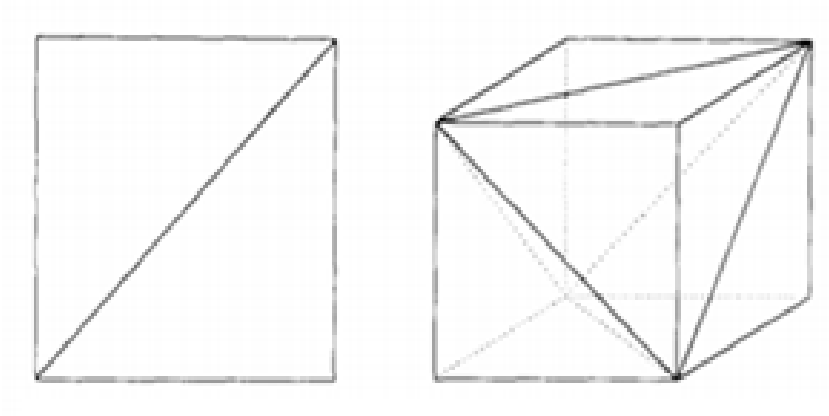

Figure 2. Conversion of quadrilateral into triangles and the brick into tetrahedral [1]

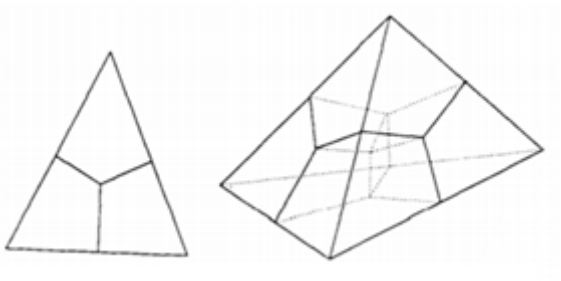

Figure 3. Conversion of triangle into quadrilaterals and the tetrahedron into bricks. A new node must be introduced in each case [1]

2.1 Classification of Meshes

Meshes are classified as Structured meshes and Unstructured meshes. The fundamental distinction in these two, is the data structures. The structured meshes produces similar shapes and the familiar two-dimension shape is the quadrilateral and three-dimension shape is the hexagon. A mesh can be classified as the structured, on a condition that the internal points are attached individually with the neighbours from the position. The unstructured meshes is completely converse to these structured meshes. Even though the algorithm of these unstructured meshes generation was developed many years prior and few of these are put forward as commercial packages, yet these are frequently confined to the applications of mechanical engineering. But the human body is unlike engineering applications in complexity. Therefore, the contour of complicated human tissues, namely the brain and heart, must be more closely adhered to, whereas the engineering applications are usually smooth and simple surfaces. When dealing with human anatomy, understanding each part is important to identify, as the subject in which it can project the mesh is required with more precession. Computerized Tomography scans and Magnetic Resonance Imaging have non-identical approach in generating the meshes and the meshes generated depicts the different views of the same object. The simple surface is initially transformed into triangulation, so that it could be utilized as an input for three-dimensional tetrahedral mesh generation algorithm [2, 11].

Structured hexahedral meshes are hardly accepted or restricted to easy geometries. Tetrahedral (unstructured) meshes require higher resolution when compared to structured meshes to gain independency of meshes, with the more computational cost (due to memory and time for computation). In the applications of Finite Elements, it's familiar that unstructured meshes (i.e., tetrahedron, wedge elements) could generate acceptable displacement results. However, generally they don't give accurate results since they are stiff shapes [12-14].

Figure 4. (a) Domain (b) Meshed domain [2]

Unstructured mesh approaches have been used in wide range of applications in computational filled simulations and these simulations could be performed with reasonable computational accuracy and cost. For these volume mesh generations, isotropic tetrahedral meshes are widely used for the inviscid and the low Reynolds number viscous flows, structural/fracture analysis, etc. due to the simplicity in terms of the generation of meshes. Recovery of boundary is another issue that is required in the Delaunay approach. The empty sphere property doesn't verify that the surface boundary preserves the original connectivity. Sometimes the constrained Delaunay approach can't be easily extended to three dimensional complex domains. It requires to produce a set of volume meshes for the multi-connected domains. Combinational advantage of the Delaunay and advancing front methods is that they are widely used. This is utilized as background meshing. New nodes are then introduced by using the advanced front strategy. The merged strategy could shorten runtime and generate meshes of high quality [15].

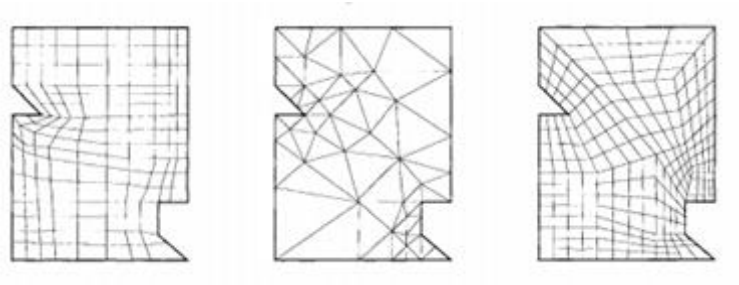

Figure 5. (a) Structured (b) Unstructured (c) Block-structured [17]

These Polygon meshes are generally utilized in the computer graphics-based implementation and in the numerical applications. In fact, these also provide the upper hand of representing as accurately as required in topology and object geometry. In addition, polygonal meshes are often known as the ideal format for data exchange (in contrast to every other computer-based design file, this is much more workable). Reproducibility and Automation are the two main features that these tools provide the clinical expertise [3, 16].

The structured and unstructured meshes commonly expands into elements. Traditionally, double-dimensional and structured meshes use quadrilateral, whereas unstructured meshes use triangles. The analog product types are hexahedral, which means topological cubes, and tetrahedra in three dimensions. However, the use of various element forms is not a basic explanation for formal and unstructured meshing. Indeed, elements can be subdivided to transform between tetrahedra and hexahedra, and between triangles and quadrilaterals (Figure-5) [17].

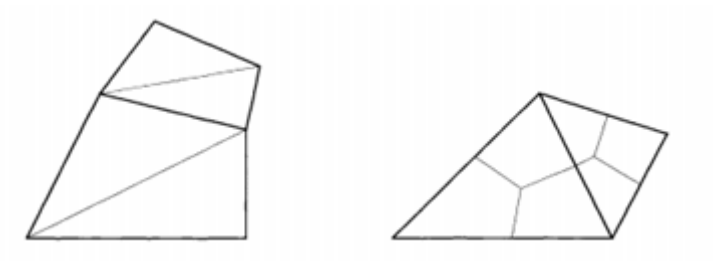

Figure 6. (a)Triangulated quadrilaterals. (b) Subdividing triangles to from quadrilaterals [17]

2.1.1 Structured two-dimensional meshes

The structured mesh is designed to be simple and practical. A structured mesh requires substantially less storage than an unstructured mesh with the same number of components, so that array storage implicitly recognizes neighbouring connectivity. An organized mesh will also save time: program quickly raises or decreases array indices while calculating a finite difference stencil. Compilers produce very powerful code for these processes; they can simplify the code for vector machines, in particular. A standardized mesh for a complex geometric domain, on the other hand, may be hard or impossible to calculate. Moreover, with this same problem, a structured mesh can need far more elements than an unstructured mesh, since elements cannot measure as quickly in size in a structured mesh. The hybrid structured/unstructured solution that decomposes a complex domain into blocks that help structured grids will solve these two problems. However, hybrid methods are not fully automatic yet and require input from the consumer when breaking down. It takes weeks or even months to work with a complex three-dimensional hybrid mesh. Hybrid method is normally late in the design cycle [17, 18].

2.1.2 Unstructured two-dimensional meshes

The advantages of unstructured meshes have already been established, including the versatile fitting of complex domains, easy degradation of small to large elements and

comparatively straightforward refinement. In contrast to structured mesh development, unstructured mesh generation appears to be one of the key computational geometry for several years at present, and a wide literature is available on this topic. Three major approaches are considered for unstructured mesh development, which use the triangulation of Delaunay, restricted triangulation of Delaunay and quadrants [17, 19].

2.2 Mesh Smoothing

Often elements generated by automatic mesh generator are not shaped well enough, but it is helpful to apply a mesh smoothing method to enhance the mesh. The mesh is refined in this process, resulting in three methods being combined at the end of the process: a) node removal; b) angle-based node smoothing to optimize node locations; and c) Delaunay refinement to optimize the connectivity of nodes. These three methods are applied in order. The angle-based node smoothing and the Delaunay refinement are applied three times consecutively [15, 20].

2.2.1 Node removal

During the generation process of these tetrahedral meshes, some nodes may be allotted to small numbers of elements as in Figure-7. Nodes looks like a tetrahedron if its neighbours are four (Figure 7a) or a pyramid if its neighbours are six (Figure-7b). Since the neighbours of these nodes are often too low-quality tetrahedral, these nodes can be removed without any conditions [15, 21].

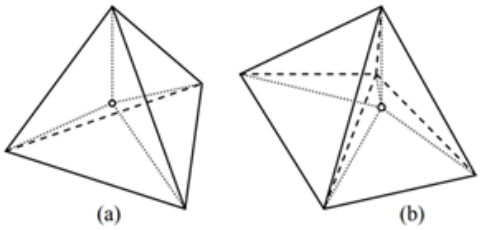

Figure 7. Nodes having 4 and 6 neighbours. [15]

2.2.2 Angle-Based Node Smoothing

An angle-based smoothing method improves mesh quality by shifting node positions. Laplacian smoothing is often employed for enhancing mesh quality because it requires a low computational cost. However, it does not guarantee to improve mesh quality and often creates

lower quality or invalid elements. The size and shape of mesh quality after the angle-based node smoothing method is much better than that after the Laplacian smoothing [15, 22].

2.2.3 Delaunay Refinement

Delaunay refinement has a strong mathematical background, and it improves the quality of meshes significantly. Considering this approach, most of the low-quality elements are caps and silvers [15].

Although a mesh is clarified, few elements are further divided into smaller pieces, but the others remain same. A triangle could be further spilt into two compact ones by bisecting the lengthy side of triangular mesh. But the diagonal transpose method can be applied during the refinement operation to produce a Delaunay Triangulation [1]. There are a set of nodes and elements in the mesh generator output. These nodes are first produced and then they are joined to form a quadrilateral or triangular element [1, 23].

Image analysis in biomedical field has a conveyer that conveys meshing image [15]. The initial step in producing meshes is to carry out image processing. The images illustrated can be similar to computed tomography, magnetic resonance imaging or X-rays. Afterwards, the principal mesh geometric models are created, starting all the way back to the meshing surface and then translating it into three-dimensional images. Information from this last stage is later used to conduct simulation and then the result is biophysical data analysis [2, 24].

2.3 Mesh Quality Inspection

The quality of the mesh should be estimated prior using them for computational analysis. The equi-angle skew and the scaled Jacobian are most common of these metrics available as the measure of mesh efficiency for the CFD and Finite Element Analysis applications [14, 25].

Initially the codes are developed in FORTRAN to produce the segmented two-dimensional medical based images. These are utilized to perform the three-dimensional regeneration of voxel-based geometries which in turn are utilized to produce the Finite Element mesh [14]. In generating the surface mesh, there are a large range of techniques using either software tools or manual/traditional methods. Few of these current software tools such as ScanIP could spontaneously generate meshes. A Simplewire software tool provides an environment for image processing by rapidly changing the three-dimensional image data taken

from Magnetic Resonance Imaging, Machine Tomography, Micro-Computer Tomography, etc. into computer models. Materialize Interactive Medical Image Control System is broadly utilized for the generation of mesh. It is a three-dimensional medical imaging program that can generate three-dimensional image data by segmentation, surface meshing. Some other popular automatic mesh generation softwares are NetGen, Gmsh, CUBIT Mesh, and TetGen. BioMesh3D is also a technology that focuses on the development of biomedical image meshes as per the research by the University of Utah [2].

2.4 Surface Mesh Generation

Surface Mesh generation is a method to distinguish a domain in order to perform numerical simulations in smaller components. It is often referred to as a mesh of two dimensions. The image quality is another significant criterion for the surface meshing. Isocontouring is a very important and useful tool in establishing surface data and also a popular technique in generating isosurfaces in marching-cube algorithm [2, 26].

A mesh surface can be designed using the edge points in parametric coordinates directly on a parametrical domain. Edge points in the parametric coordinate system can be created through the binary edge subdivision. In order to represent the entity size specifications, a point separation function should be employed during internal point formation in the parametric domain in physical space [18].

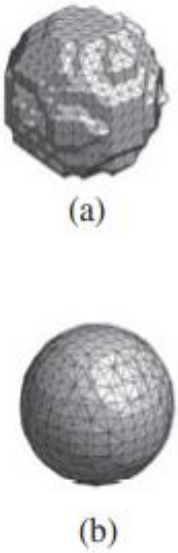

Figure 8. Surface mesh of a sphere [19]

2.5 Volume Mesh Generation

The volume mesh generation includes the formation of tetrahedral elements using the restricted Delaunay process. In this step, to comply with the metric map given, the surface mesh is stored and the mesh elements are loaded into the domain. For the purpose of simulation, these component shape characteristics are given considerable attention. In the mid-eighties, the "Marching Cubes" algorithm was developed as an automated instrument for implicit discrete surface reconstruction [3].

With the support of the so-called Delaunay Kernel, each vertex of this surface triangulation is loaded into the primary mesh. The missing surface triangles are mainly perked up at the final state with the aid of the edge and the flip-ping operations of the face. And after that the internal vertices are fabricated and loaded with the aid of a similar process into these meshes. To terminate this, it is possible to implement a discreet metric tensor described in the earlier stages and then to consider whether they should be held together or spread out on the existing mesh edges [3].

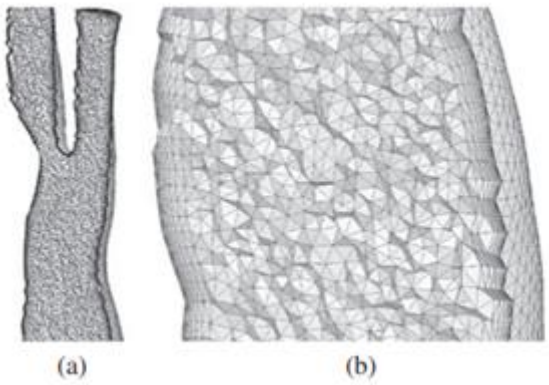

Figure 9. (a) Volume mesh cut-off (b) Zoomed view cut-off [19]

2.6 Tetrahedral Mesh Generation

The outline of the Tetrahedral Mesh generation process is shown in Figure-10. From the initial front definition by the surface mesh, tetrahedral elements are created inside these domains. To avoid these complications in front, tetrahedral elements are produced by each layer which is the base front. In this type of approach, background meshes are not required for tetrahedral mesh generation to simplify the procedure. At each node in the nth level front, a region of influence will be considered. The user description for the tetrahedral elements is water tight triangular surface mesh and detention factor [15].

The background mesh for the simplification process is not required for the generation of tetrahedral mesh. Each node in the influence region is considered as a n-level front. The user input is considered as water-tight triangular surface mesh and a stretching factor for tetrahedral elements [15].

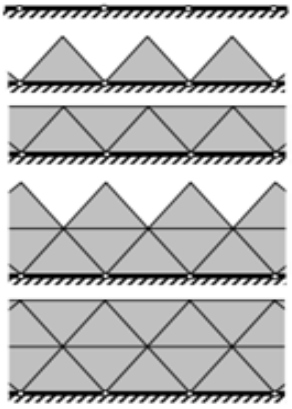

Figure 10. Tetrahedral mesh generation process [15]

Smoothing is also an important factor not to create too big or small elements and to prevent the generation of mesh from falling. For example, in Figure-11, the tetrahedral meshes from low-quality meshes which have large-sized jumps and silvers are just for demonstration. Owing to the height smoothing, triangles that are appearing on cross-section are uniform locally [15].

2.7 Applications

In the last few years, medical imaging equipment has developed from pure diagnostic technique to many uses, including patient-specific tooling and implants, mathematical simulation or studies into joint cinema. It was used to produce a three-dimensional (3D) anatomy model of the patient, using CT or MRI data [20].

Background meshes for these surface triangulations are brought out from Computerized Tomography/Magnetic Resonance Imaging data to represent fidelity models. These tetrahedral mesh generation process has been applied to pelvic bone and skull/brain models [15].

2.7.1 Simplified Skull/Brain Model

Computational simulations for the traumatic brain injury are required to understand how it occurs, for example: To develop safer cars. A set of these meshes for the simplified skull/brain model is shown in Figure-12. Major components of head are brain (white and grey

matters), cerebrospinal fluid, skin and bone (skull and spine). The modelling of cerebrospinal fluid is very important because it acts as a cushion for a blow to the head and decreases the impact. In this case, meshes are produced for the brain, the skull, and the region between the brain and skull. An advancing front method preserves the connectivity of the surface boundaries. Even if three tetrahedral meshes are produced for three different domains, the corresponding surface boundaries are identical. Figure-13 shows the asymmetry of these tetrahedral for three meshes. Even if the outermost two layers have narrow volumes, the quality of these elements are acceptable [15].

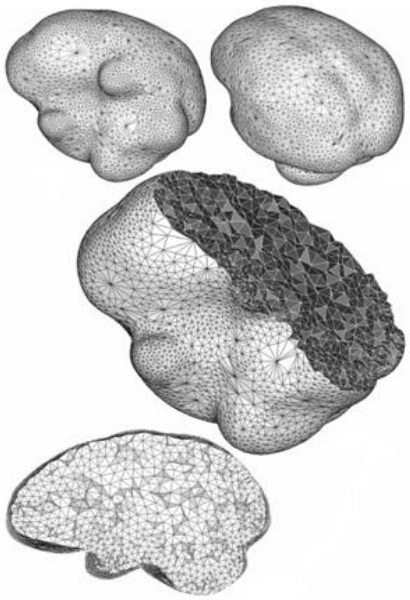

Figure 11. Tetrahedral meshes from low-quality meshes which have large-sized jumps and silvers [15]

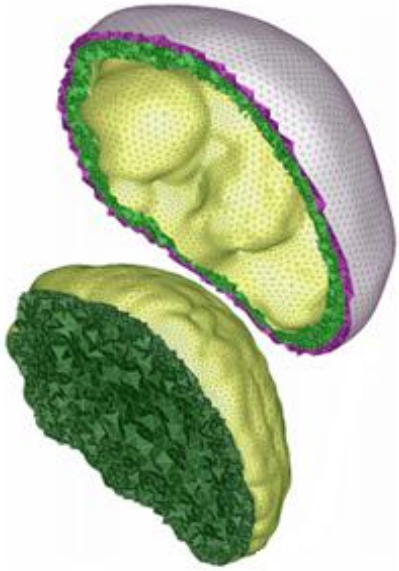

Figure 12. Meshes for the simplified skull/brain model [15]

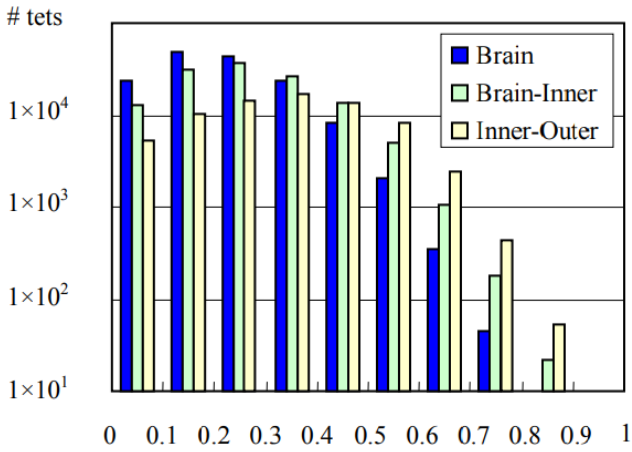

Figure 13. Skewness of the tetrahedral in the simplified brain/skull model [15]

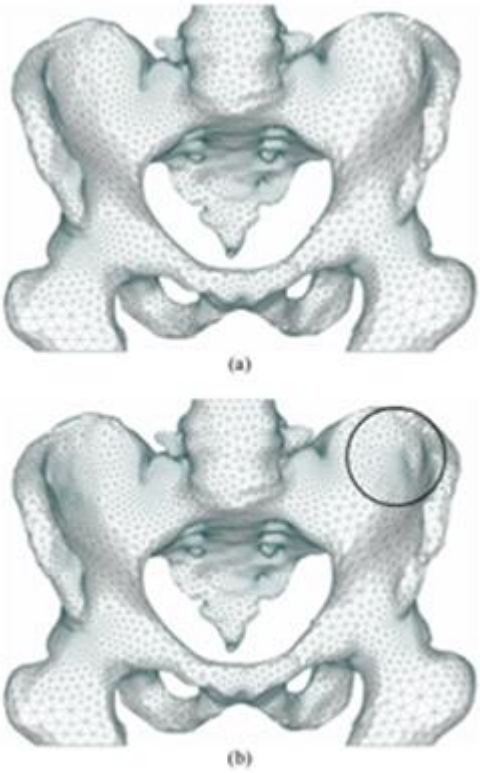

Figure 14. Surface mesh generation for a human pelvis bone: (a) original; (b) after refinement considering the thickness of the volume [15]

2.7.2 Human Pelvis Bone

To probe the injury of human bones, mesh generation from Computation Tomography/ Magnetic Resonance Imaging data is essential to carryout realistic simulations. Figure-14 manifests surface meshes for the human pelvis bone. The quality of the native surface mesh is magnificent, if the volume mesh is generated outside. In actual numerical simulations, decreasing the number of elements is sometimes essential, but the quality of these volume meshes is also very important. To create a finer volume mesh, the surface meshes are refined in view of local thickness of volume prior hand [15].

2.8 Comparison between MRI and CT scan

Computerized tomography (CT) is the gold standard for scanning bones to create 3D models with high geometric accuracies. CT scanning of healthy people is not morally sound due to the high degree of radiation exposure. Studies of CT imaging protocols using low dose radiation have been an important aspect of scientific science thus maintaining the original image quality. However, sensitivity to radiation cannot be avoided entirely. In addition, certain

countries do not allow healthy volunteers to be screened with radiation of any kind (low or high dosage) except for medical purposes. MRI is used for scanning high image quality soft tissues for the pure use of anatomical 3D models. The MRI is best suited for proton (1H) nuclei scanning of soft tissues as the signal source. MRI is not consistently used for bone scanning because, in a very short 1H transverse relaxation cycle, the bone tissue does not provide an RM signal (T2). However, with the signal produced from the adjacent soft tissue, the bone cortex geometry can be described (Figure-15). The key benefit of using MRI is that it does not require ionizing radiation and is also suitable for screening of healthy human volunteers [22].

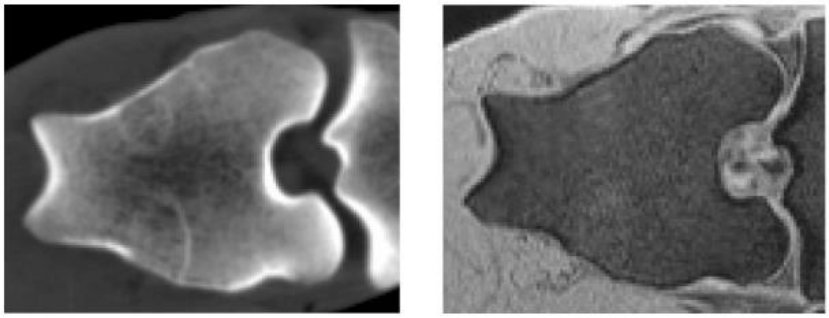

Figure 15. CT (left) and MRI (right) of knee joint

Figure-15 shows the axial slices (the proximal end of the tibia is also visible on the right side of the images as the limb has been scanned with flexed knee joint) from the distal region of the femur. Cortical bone does not generate an MRI signal and appears in black while this is clearly visible in the CT image. Parts of the trabecular structure are visible due to the presence of bone marrow.

The models were registered in two phases in order to compare 3D models based on the MRI and the CT, by aligning their axis of inertia and by a global ICP registration. The optical scan calculated the distance between the vertices of the optical scanner and the reconstructed 3D objects, relative to the 3D image model of the bone, where a positive distance means that the optical scan is larger than the image-based model. Different parameters have been calculated from this series of error measurements: mean error and default variance, mean and uniform error deviation, root-mean sq. error and the 95 percent absolute, and undeclared error value. The value of 95 percent gives a reasonable approximation of the overall 3D model geometric precision and ignores potential outlines in the dataset. After registration, the optical scans were also divided into three parts to compare different regions with 3D models, as seen in the Figure-16. The goal is to explore whether various geometries of diaphyseal and epi-physical regions of the bones contributed to the re-constructed 3D model having different

accuracies. As the size of the knee spindle was small, the MRI 3D model is based only on the proximal epiphysis and the proximal portion of the diaphysis. To assess the effect of the tissue movement protocol on the surface bone layer, the models resulting from different CT scans were also compared [20].

Figure 16. In reference to the 3D reconstruction of the bones, the optical scam was divided into three parts: A represents the preaximal epiphysis of the tibia, described as the most preaximal 10% of the bone, B the diaphyseal portion and C the disease epiphysis, classified as the most distal 10% of the bone [20].

2.9 Higher-order Mesh Generation

Higher-order mesh generators are known for better numerical solution accuracy. The literature includes many higher-order mesh generators, such as Gmsh [9], Mesh Curve [10], HOmesh2D [11], HOtetramesh [13], etc. In biomedical applications, these meshes can be used to enhance the precision of the solution. In addition, using the sub parametric meshes [11-13], the numerical solution efficiency can be improved using the subparametric higher-order finite element method.

3. Results

A comparison between the multi-threshold CT-based models and the reference models (Contact Scanner-based Models) showed that the average error of both models are 0.15 mm (Figure-17). The MRI-based 3D models showed a 0.23 mm average defect relative to the reference models (Figure-18). When comparing MRI models with CT-based models, a mean-age error of 0.23 mm is established. Average CT and MRI variant differences ($p = 0.067$) are not statistically relevant [22].

The diaphyseal regions have the lowest mean error of 0.07 mm and 0.15 mm, respectively, relative to the related reference models, when different CT-based and MRI-based 3D regions were presented (Figure-19) [22].

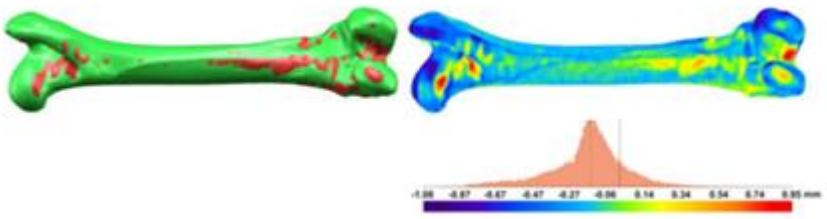

Figure 17. The final 3D model generated from MRI data (red) aligned with reference model (green) on left and comparison of the surface geometry of those two models on right [22]

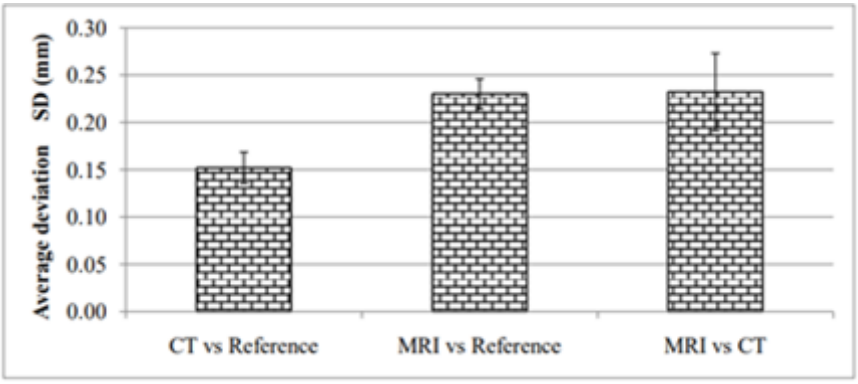

Figure 18. The average deviation between CT vs reference, MRI vs references and MRI vs CT based 3D models [22]

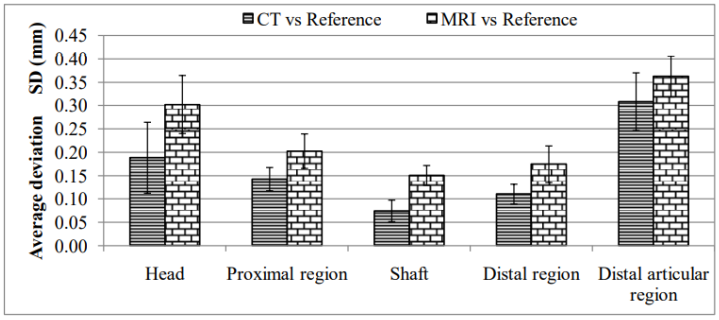

Figure 19. Comparison with reference model of various anatomical regions of CT and MRI models [22]

Based on the results, the comparison model was underestimated by 50.9% for surfaces of CT models and by 78.8% for MRI models, while CT models were underestimated by 75.8% for surfaces of MRI models (Table 1). In their proximal, diaphyseal and distal territories, CT modelling overestimated the reference models while they were underestimated by reference models in the same MRI regions.

Table 1. CT and MRI models surface percentages that under or overestimate the reference model and the MRI model area percentage that underestimates or overestimates the CT model [22].

	Whole bone	Head	Proximal region	Diaphysis	Distal region	Distal articular region
CT vs Reference	-50.9%	-80.9%	66.8%	60.6%	58.2%	-84.4%
MRI vs Reference	-78.8%	-81.8%	-70.5%	-93.8%	-68.8%	-75.2%
MRI vs CT	-75.8%	-62.2%	-79.7%	-95.2%	-71.6%	-54.9%

Negative values indicate that the model of interest underestimates the reference model

Statistically, there were substantial variations between CT and MRI models based on the multi-threshold approach (p=0.008) between distal regions (Table 2).

Table 2. Statistical significance between CT vs reference average deviations and MRI vs reference models [22].

Region	Significance
Head	p = 0.065
Proximal region	p = 0.478
Diaphysis	p = 0.435
Distal region	p = 0.008
Distal articular region	p = 0.697

4. Conclusion

The present study comprehensively investigates the various types of meshing techniques available in the biomedical field. This enhances the way organs in human anatomy are examined. Technology is evolving rapidly which makes human life easier and comfortable. Likewise, this emerging technology can enable us to solve health problems and life-threatening biological problems. Meshes aid a great deal in engineering applications to model items for testing purposes in order to produce better products. In a similar way, meshing in biomedical applications allows to study the internal organs of the human body more accurately and effectively to solve the problems. Using the sub parametric higher-order finite element approach, the solution accuracy and efficiency of these problems could be further improved. It takes raw medical imaging data, then processes it and generates a 3D model of the organ required to analyse and find solutions that are far more accurate and simpler than traditional approaches.

References

[1] Ho-Le, K., 1988. Finite element mesh generation methods: a review and classification. Computer-aided design, 20(1), pp.27-38.

[2] Alias, S., Abas, Z.A., Shibghatullah, A.S. and Rahman, A.F.N.A., 2014, November. A BRIEF REVIEW OF SURFACE MESHING IN MEDICAL IMAGES FOR BIOMEDICAL COMPUTING AND VISUALIZATION. In International Symposium on Research in Innovation and Sustainability 2014.

[3] Pagès, A., Sermesant, M. and Frey, P., 2005, September. Generation of computational meshes from MRI and CT-scan data. In ESAIM: Proceedings (Vol. 14, pp. 213-223). EDP Sciences.

[4] Magne, P., 2007. Efficient 3D finite element analysis of dental restorative procedures using micro-CT data. Dental materials, 23(5), pp.539-548.

[5] Jermyn, M., Ghadyani, H.R., Mastanduno, M.A., Turner, W.D., Davis, S.C., Dehghani, H. and Pogue, B.W., 2013. Fast segmentation and high-quality three-dimensional volume mesh creation from medical images for diffuse optical tomography. Journal of biomedical optics, 18(8), p.086007.

[6] Callahan, M., Cole, M.J., Shepherd, J.F., Stinstra, J.G. and Johnson, C.R., 2009. A meshing pipeline for biomedical computing. Engineering with Computers, 25(1), pp.115-130.

[7] C. Geuzaine, J.-F. Remacle,Gmsh: a three-dimensional finite element mesh generator with built-in preand post-processing facilities, International Journal for Numerical Methods in Engineering 79(11)(2009) 1309-1331.

[8] Jeremy Ims, Zhaowen Duan, Zhi J. Wang, meshCurve: An Automated Low-Order to High-Order Mesh Generator, 22nd AIAA Computational Fluid Dynamics Conference, AIAA AVIATION Forum, (AIAA 2015-2293) (2015).

[9] Smitha, T.V., Nagaraja, K.V. and Jayan, S.,. MATLAB 2D higher-order triangle mesh generator with finite element applications using subparametric transformations. Advances in Engineering Software, 115, pp.327-356, 2018

[10] Smitha, T. V., and K. V. Nagaraja. "Automated higher-order mesh generation in MATLAB on biomaterials." In IOP Conference Series: Materials Science and Engineering, vol. 577, no. 1, p. 012130. IOP Publishing, 2019.

[11] Smitha, T. V., and K. V. Nagaraja. "MATLAB automated higher-order tetrahedral mesh generator for CAD geometries and a finite element application with the subparametric mappings." Materials Today: Proceedings (2020).

[12] De Santis, Gianluca, Matthieu De Beule, Koen Van Canneyt, Patrick Segers, Pascal Verdonck, and Benedict Verhegghe. "Full-hexahedral structured meshing for image-based computational vascular modeling." Medical engineering & physics 33, no. 10, pp.1318- 1325, 2011.

[13] Ito, Yasushi, Alan M. Shih, and Bharat K. Soni. "Reliable isotropic tetrahedral mesh generation based on an advancing front method." In IMR, pp. 95-106. 2004.

[14] Audette, M. I. C. H. E. L. A., Andrey Chernikov, and Nikos Chrisochoides. "A review of mesh generation for medical simulators." Handbook of Real-World Applications in Modeling and Simulation 2, 261, 2012.

[15] Mesh Generation Marshall Bern Xerox Palo Alto Research Center, 3333 Coyote Hill Rd., Palo Alto, CA 94304 E-mail: bem @parc.xerox, com Paul Plassmann* Department of Computer Science and Engineering, The Pennsylvania State University, University Park, PA 16802 E-mail: plassman@cse.psu.edu

[16] Lewis, R.W., Zheng, Y. and Gethin, D.T., Three-dimensional unstructured mesh generation: Part 3. Volume meshes. Computer Methods in Applied Mechanics and Engineering, 134(3-4), pp.285-310, 1996.

[17] Sazonov, I. and Nithiarasu, P., Semi-automatic surface and volume mesh generation for subject-specific biomedical geometries. International Journal for Numerical Methods in Biomedical Engineering, 28(1), pp.133-157, 2012.

[18] Van den Broeck, J., Vereecke, E., Wirix-Speetjens, R. and Vander Sloten, J., Segmentation accuracy of long bones. Medical engineering & physics, 36(7), pp.949-953, 2014.

[19] Tizzard, A., Horesh, L., Yerworth, R.J., Holder, D.S. and Bayford, R.H., Generating accurate finite element meshes for the forward model of the human head in EIT. Physiological measurement, 26(2), p.S251, 2005.

[20] Rathnayaka, K., Momot, K.I., Noser, H., Volp, A., Schuetz, M.A., Sahama, T. and Schmutz, B., Quantification of the accuracy of MRI generated 3D models of long bones compared to CT generated 3D model

[21] Balasubramaniam, Vivekanadam. "Artificial Intelligence Algorithm with SVM Classification using Dermascopic Images for Melanoma Diagnosis." Journal of Artificial Intelligence and Capsule Networks 3, no. 1 (2021): 34-42.

[22] Tesfamikael, Hadish Habte, Adam Fray, Israel Mengsteab, Adonay Semere, and Zebib Amanuel. "Simulation of Eye Tracking Control based Electric Wheelchair Construction by Image Segmentation Algorithm." Journal of Innovative Image Processing (JIIP) 3, no. 01 (2021): 21-35.

[23] Karuppusamy, P. "Building Detection using Two-Layered Novel Convolutional Neural Networks." Journal of Soft Computing Paradigm (JSCP) 3, no. 01 (2021): 29-37.

[24] Manoharan, Samuel. "Early diagnosis of Lung Cancer with Probability of Malignancy Calculation and Automatic Segmentation of Lung CT scan Images." Journal of Innovative Image Processing (JIIP) 2, no. 04 (2020): 175-186.

[25] Sungheetha, Akey, and Rajesh Sharma. "Design an Early Detection and Classification for Diabetic Retinopathy by Deep Feature Extraction based Convolution Neural Network." Journal of Trends in Computer Science and Smart technology (TCSST) 3, no. 02 (2021): 81-94.

[26] Vijayakumar, T., Mr R. Vinothkanna, and M. Duraipandian. "Fusion based Feature Extraction Analysis of ECG Signal Interpretation–A Systematic Approach." Journal of Artificial Intelligence 3, no. 01 (2021): 1-16.